V-H-M Yield Surface describing Soil Structure Interaction of Sub-sea Structures and Wind Turbines on Caisson Foundations in Soft Clays

C. Athanasiu
Multiconsult ASA, Norway, corneliu.athanasiu@multiconsult.no

M. Brandt
Multiconsult ASA, Norway, madeleine.brandt@multiconsult.no

ABSTRACT
One of the challenges in the design of sub-sea structures and wind turbines on caisson foundations is the realistic representation of foundation-soil stiffness and capacity. Such a representation can be "lumped" as load-displacement relationships at the top of the caisson (sea-bed level).
The paper presents a general V (vertical load) - H (horizontal load) - M (overturning moment) yield surface and back-bone load – displacement (H-δ_h, M-θ and V-δ_v) curves that can be used in geotechnical design of a structure and its caisson foundation. The soil parameters, together with the model formulation and limitations, are presented and discussed in the paper. The last part of the paper illustrates some of the applications of the yield surface in the design.

Keywords: soil-structure interaction, VHM yield surface, back-bone curves.

1 INTRODUCTION

An important tool for the analysis of soil-structure interaction problems, particularly of dynamic soil-structure interaction of sub-sea structures and wind turbines on caisson foundations, are discrete, "force resultant" models. In these models, the details of stresses and deformations in the soil mass and at the interface with the caisson are replaced by the force and moment resultants acting at caisson top centre (seabed level) and the resulting displacements.
The paper presents finite element analyses of caisson foundation in typical North Sea, soft clay. The results confirm the failure envelope proposed by Kay and Palix, 2011 and 2015. The envelope is extended to a yield surface using two kinematic hardening parameters, m_{HM} and m_V, the mobilization degree of lateral and of vertical loading, respectively.
The kinematic hardening rule for lateral loading is based on back-bone curves derived from force-displacement results of finite element analyses.

2 VHM FAILURE ENVELOPE AND YIELD SURFACE

2.1 Failure envelope

Large scale, field tests and small scale, laboratory tests on caisson foundations have shown that a failure envelope can be established as the locus of all load combinations, V-H-M, provided all forces and moment act in the same vertical plane passing through the top centre of the caisson (Houlsby, Ibsen and Byrne, 2005). The shape of the envelope is confirmed by numerical analyses along different load paths.
Kay and Palix, 2011, found that a caisson with diameter D and length L has an elliptical envelope,

Figure 1, expressed as:

$$H^*_{ult}(t)=a_{MH}\cdot\cos(t)\cdot\cos(\varphi_{MH})+ b_{MH}\cdot\sin(t)\cdot\sin(\varphi_{MH}) \quad (1)$$

$$M^*_{ult}(t)= a_{MH}\cdot\cos(t)\cdot\sin(\varphi_{MH})- b_{MH}\cdot\sin(t)\cdot\cos(\varphi_{MH})$$

In Eq.(1) $H^*_{ult}(t)$ and $M^*_{ult}(t)$ are the normalized horizontal ultimate force, H_{ult}/H_o and ultimate moment, M_{ult}/M_o, respectively. $H_o= D\cdot L\cdot s_{u,ave,L}$ and $M_o= D\cdot L^2\cdot s_{u,ave,L}$ are the reference force and moment respectively. $s_{u,ave,L}$ is the average undrained shear strength of soil over the length L of the caisson. The ellipse (the major axis) is rotated from horizontal by an angle of φ_{MH}. The radius connecting the origin with the current point (H^*_{ult}, M^*_{ult}) on the ellipse makes an angle t with the ellipse major axis.

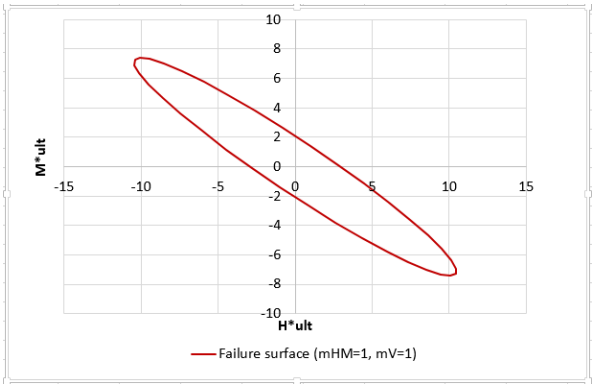

Figure 1. Failure envelope.

The coefficients a_{MH}, b_{MH} and ϕ_{MH} are presented in Kay and Palix, 2011.

2.2 Yield surface

Using the work of Kay and Palix, 2015, a general yield surface can be expressed as:

$$F=H^{*2}\cdot f(h/L)-\xi(m_V)\cdot m_{HM}^2=0 \quad (2)$$

where $m_V=V^*/V^*_{ult}$, $m_{HM}=H^*/H^*_{ult}$ $=M^*/M^*_{ult}$ during loading along M/H=h = constant load path.
The hardening function for vertical load is, according to Kay and Palix, 2015:

$$\xi(m_V) = [1-m_V^{\,bVH}]^{(2/aVH)} \quad (3)$$

with the parameters a_{VH} and b_{VH} linear functions of the ratio L/D.
The function f(h/L) is calculated as:

$$f(h/L) = [(\cos(\phi_{MH})+(h/L)\cdot\sin(\phi_{MH}))/a_{MH}]^2+ [((h/L)\cdot\cos(\phi_{MH})- \sin(\phi_{MH}))/b_{MH}]^2 \quad (4)$$

For any mobilization degree of vertical loading, m_V and of lateral loading, m_{MH}, the normalized lateral loads can be find for any loading path, h/L, as:

$$H^*=m_{MH}\cdot\sqrt{[\xi(m_V)/f(h/L)]} \quad (5)$$

$$M^*=H^*\cdot h/L$$

Finite element analyses of caisson foundation in soft clay from North Sea are performed using PLAXIS 3D to check the applicability of the failure envelope proposed by Kay and Palix. The finite element model is shown in Figure 2. The caisson foundation was modelled as a hollow cylinder using linear elastic plate elements. The cylinder has a length of L = 18.5 m and a diameter of D = 7.5 m.

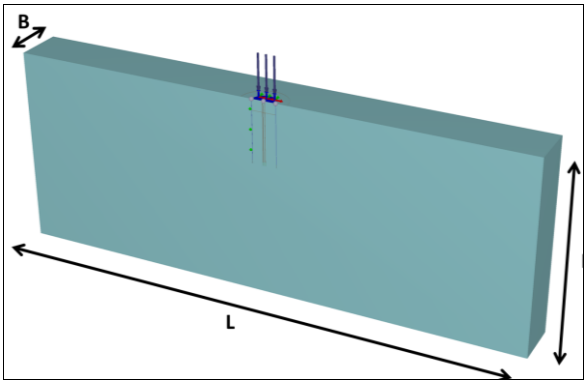

Figure 2. Finite element model.

The vertical (own weight) load, V, is applied as uniformly distributed load over the top plate of the caisson. The horizontal load, H, was applied as a point load at the centre of the caisson lid. To model the moment load, M, two equal vertical loads in opposite direction of each other were applied at the edge of the caisson lid. Both H and M were applied simultaneously in undrained conditions. In each analysis, the ratio, h=M/H, was kept constant (a linear load path in the M-H plot). The combined loading

phase, H and M, was performed by incrementally increasing the loads with a specific maximum load fraction per step until failure occurred.
The soil is modelled using "Undrained B" Mohr-Coulomb model. The soil parameters are described in Table 1. The results of PLAXIS 3D analyses are plotted together with the yield surface, Eq. (2) for m_V=0.5

Table 1. Soil parameters

Parameter	Units	Value
Identification	-	MC clay
Material Model	-	Mohr-Coulomb
Drainage type	-	Undrained (B)
γ	kN/m3	16.4
E	kN/m2	2575
ν	-	0.35
c_{ref}	kN/m2	1.87
E_{incr}	kN/m2/m	2788
z_{ref}	m	0
c_{incr}	kN/m2/m	2.025
z_{ref}	m	0
Tension cut-off	-	Yes
Tensile strength	kN/m2	0
R_{inter}	-	0.5
k_o	-	0.6

and m_{MH}=1 (failure in lateral loading) in Figure 3.a and b.
As can be seen from Figure 3, the yield surface is in good agreement with the results from PLAXIS 3D analyses on soft, North Sea clay.

3 FORCE-DISPLACEMENT BACK-BONE CURVES

The force-displacement and moment-rotation curves from PLAXIS analyses were used to derive expressions for back-bone curves providing the kinematic hardening rule of the yield surface in monotonic loading.
For each loading path with constant load ratio, h=M/H, back-bone curves H-δ and M-θ, are described using the initial stiffness parameters, $K_{\delta max}$ and $K_{\theta max}$, as functions of h/L, and secant stiffness degradation with displacement.

3.1 Initial stiffness

The initial stiffness of back-bone curves vary with the loading path ratio, h/L as shown in Figure 4. The variation of initial stiffness with the loading path ratio h/L is found to be described by:

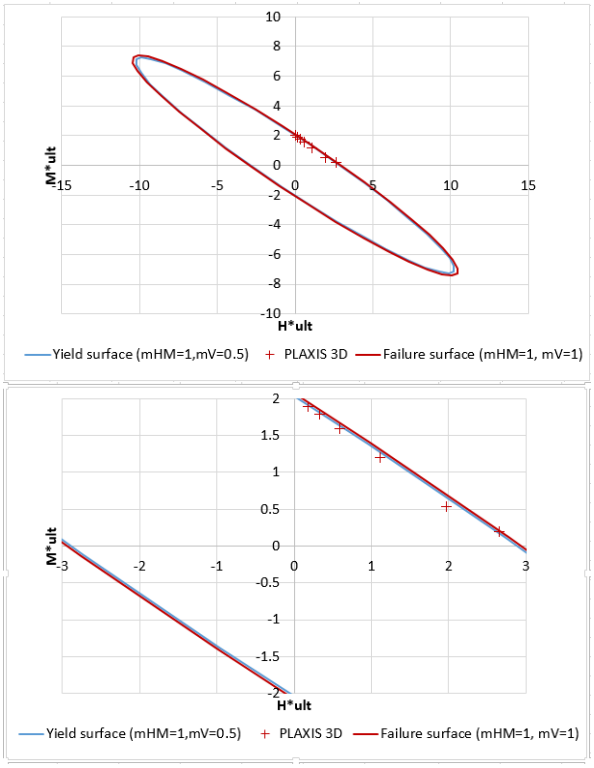

Figure 3 a. Yield surface and PLAXIS 3D results. b. Detail of Figure 3.a.

$$K_{\delta\delta max}=K_{\delta\delta max,max}-k_{1\delta}\cdot x/(1/k_{o\delta}+k_{2\delta}\cdot x/(K_{\delta\delta max,max}-K_{\delta\delta maxo}))$$

$$\text{with } x=\log(h/h_o),\ h_o=0.1\cdot L \qquad (6)$$

Similarly:

$$K_{\theta\theta max}=K_{\theta\theta max,o}+k_{1\theta}\cdot x/(1/k_{o\theta}+k_{2\theta}\cdot x/(K_{\theta\theta max,max}-K_{\theta\theta maxo})) \qquad (7)$$

The coefficients $k_{1\delta}\ldots k_{o\theta}$ are found by curve fitting technique.
The "boundary" stiffness, $K_{\delta\delta max,max}$ is the initial, elastic stiffness for load path ratio h_o/L and $K_{\delta\delta max,o}$ corresponds to load path ratio h_{ult}/L (h_{ult}=1000m). The "boundary" stiffness for rotation, $K_{\theta\theta max,o}$ corresponds to h_o/L and $K_{\theta\theta max,max}$ to h_{ult}/L. The boundary stiffness can be determined by using elastic solutions for caisson stiffness.

For a caisson embedded in elastic soil with soil reaction coefficient varying linearly with depth, k=m·z, the following stiffness relations can be written for soil lateral reactions on the caisson:

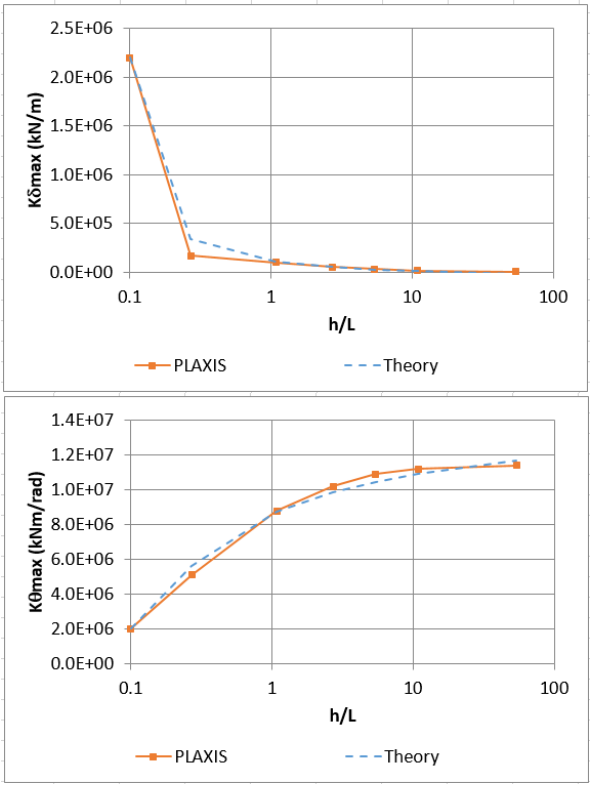

Figure 4 Variation of initial stiffness with h/L

$$H_{lat}=m\cdot D\cdot L^2/2\cdot\delta + m\cdot D\cdot L^3/3\cdot\theta$$
$$M_{lat}= m\cdot D\cdot L^3/3\cdot\delta+ m\cdot D\cdot L^4/4\cdot\theta \quad (8)$$

Using solutions from Gazetas, 2005, the coefficient m can be expressed as a function og G_{max}/s_u as follows:

$$m=2/(1-\nu)\cdot(G_{max}/s_u)\cdot(s_u/p_o')\cdot\gamma'/D \quad (9)$$

Similarly, the stiffness of bottom soil reactions can be expressed using Gazetas equations as:

$$H_{bot}=K_{xb}\cdot\delta+K_{x\theta b}\cdot\theta$$
$$M_{bot}= K_{x\theta b}\cdot\delta+ K_{\theta b}\cdot\theta \quad (10)$$

where:

$$K_{xb}=8\cdot G_b\cdot R/(2-\nu),\ K_{\theta b}=8G_bR^3/3(1-n) \text{ and}$$
$$K_{x\theta b}=(8\cdot G_b\cdot R/(2-\nu)- m\cdot D\cdot L^2/2)\cdot L/3 \quad (11)$$

The total initial stiffness is obtained from the equilibrium of lateral and bottom reaction with the applied force and moment:

$$H=H_{lat}+H_{bot}= K_h\cdot\delta+K_{h\theta}\cdot\theta$$
$$M=M_{lat}+M_{bot}-H_{bot}\cdot L= K_{h\theta}\cdot\delta+ K_\theta\cdot\theta \quad (12)$$

The Eqs.(12) can be written as flexibility equations:

$$\delta=(H\cdot K_\theta-M\cdot K_{h\theta})/\Delta=[(K_\theta-h\cdot K_{h\theta})/\Delta]\cdot H$$
$$\theta=(M\cdot K_h-H\cdot K_{h\theta})/\Delta=[(K_h-(1/h)\cdot K_{h\theta})/\Delta]\cdot M$$
$$\Delta=(K_h\cdot K_\theta-K_{h\theta}^2) \quad (13)$$

The boundary stiffness can now be determined from eq.(13), by selecting h equal to h_o or h_{ult} as explained before.
The boundary stiffness were determined using the ratio su/po'=0.32 as results from PLAXIS input and a ratio G_{max}/s_u=1000, in Eqs.(8)…(13). The values had to be corrected by adjusting coefficients (0.02-0.03 for rotation stiffness and 1.5-1.9 for displacement stiffness) in order to match the PLAXIS results, probably due to the influence roughness used for interface elements and other 3D effects.

Using the corrected values for boundary stiffness and the Eqs.(6) and (7) for initial stiffness a good agreement is shown between PLAXIS and predicted stiffness (Fig.4).

3.2 Kinematic hardening rule for lateral loading

The kinematic hardening rule is described by the back-bone curves force-displacement and moment-rotation using the formulation proposed by Athanasiu et al., 2008:

$$H=(K_\delta/K_{\delta max})\cdot(\delta/\delta_r)\cdot H_{ult}$$
$$M=(K_\theta/K_{\theta max})\cdot(\theta/\theta_r)\cdot M_{ult} \quad (14)$$

with:

$$K_\delta/K_{\delta max}=1-c_{1\delta}\cdot\text{atan}\{\exp[c_{2\delta}\cdot\log(\delta/\delta_i)]\} \quad (15)$$
$$K_\theta/K_{\theta max}=1-c_{1\theta}\cdot\text{atan}\{\exp[c_{2\theta}\cdot\log(\theta/\theta_i)]\}$$

In eqs. (14) and (15), K_δ and K_θ are the secant stiffness corresponding to displacement δ and rotation θ, respectively. $K_{\delta max}$ and $K_{\theta max}$ are initial stiffness parameters. δ_r and δ_i are reference displacement, H_{ult}/ $K_{\delta max}$ and displacement at inflexion point on the curve $K_\delta/K_{\delta max}$ vs. log(δ). The coefficients $c_{1\delta}$ and $c_{2\delta}$ are determined from the ratio $K_{\delta ult}/K_{\delta max}$ and from the slope of the curve $K_\delta/K_{\delta max}$ vs. log(δ) at the inflection point.
Examples of predicted back-bone curves as compared to PLAXIS results are shown in Figure 5.

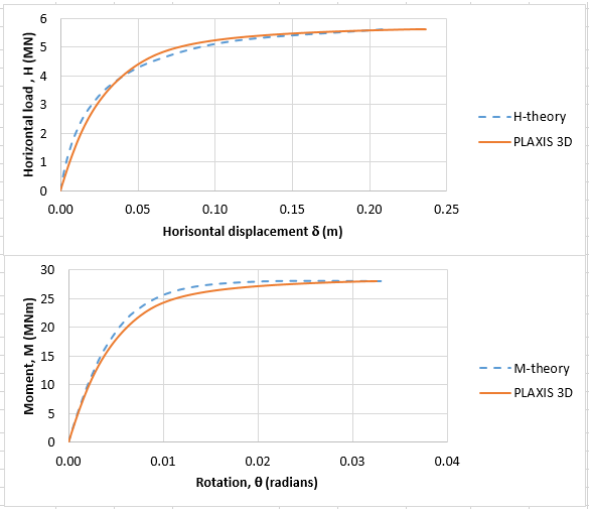

Figure 5. Back-bone curves

The kinematic hardening rule for lateral loading relating the kinematic hardening parameter, $m_{HM=}$ $(K_\delta/K_{\delta max})\cdot(\delta/\delta_r)$ with plastic displacements $\delta_{pl}=H/ K_{\delta max}\cdot[1/(K_\delta/K_{\delta max})-1]$ is determined from back-bone curve (Figure 6).

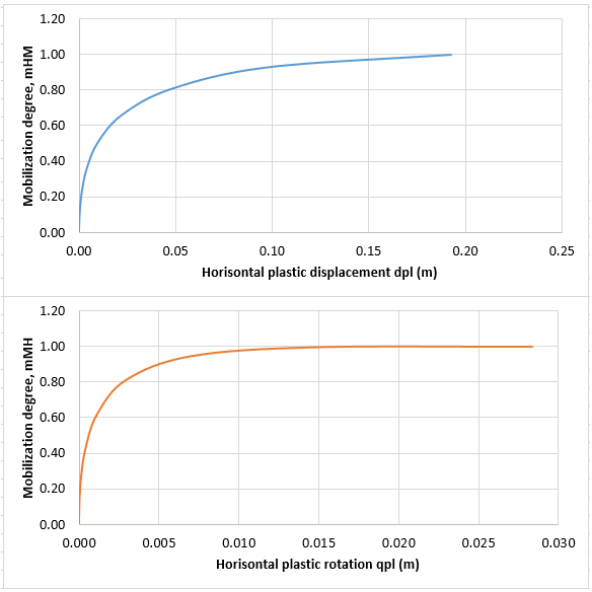

Figure 6. Kinematic hardening rule.

4 APPLICATION OF THE YIELD SURFACE AND BACK-BONE CURVES

4.1 Estimation of safety factor to failure

The key application of the yield surface for mobilization degree $m_{HM}=1$ (failure envelope) is that the envelope allows an explicit consideration of the independent load components and a graphical interpretation of the factor of safety associated with different load paths.
Consider as an example the loading situation in Figure 7. The loading path for permanent load is OA and for environmental loads is represented by the segment AB. Using the definition from ISO 19991-4, the safety factor is SF=AC/AB=1.73. The conventional bearing capacity verification would look at the ratio between vertical bearing capacity including the effect of horizontal load and the total applied vertical load: SF_{conv}= DE/DB=1.56.

4.2 Dynamic soil-structure interaction analyses in frequency domain

The back-bone curves provided by the model are used with a variable secant stiffness procedure in a modal analysis of a sub-sea structure. A loading ratio, h and secant

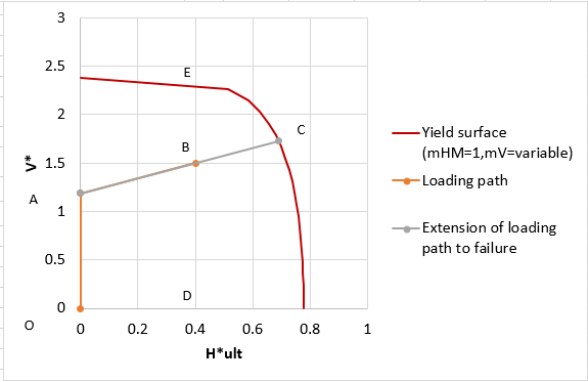

Figure 7. Definition of safety.

stiffness's K_δ and K_θ are initially assumed and a modal analysis is performed. A first estimate of natural frequencies and periods, ω_n and T_n, of dynamic loads, H_{EQ} and M_{EQ} and of displacements, δ_{EQ} and θ_{EQ} as a function of pseudo response acceleration, $PSa(T_n)$, is obtained.
The process converges only if:

- the dynamic stiffness's are compatible to the soil-caisson response stiffness described by back-bone curves;
- The dynamic load ratio $h_{dyn}=M_{EQ}/H_{EQ}$ is the same as the assumed ratio, h;
- The same mobilization degree $m_H=H/H_{ult}=M/M_{ult}$ is obtained for both, dynamic moment and dynamic force;

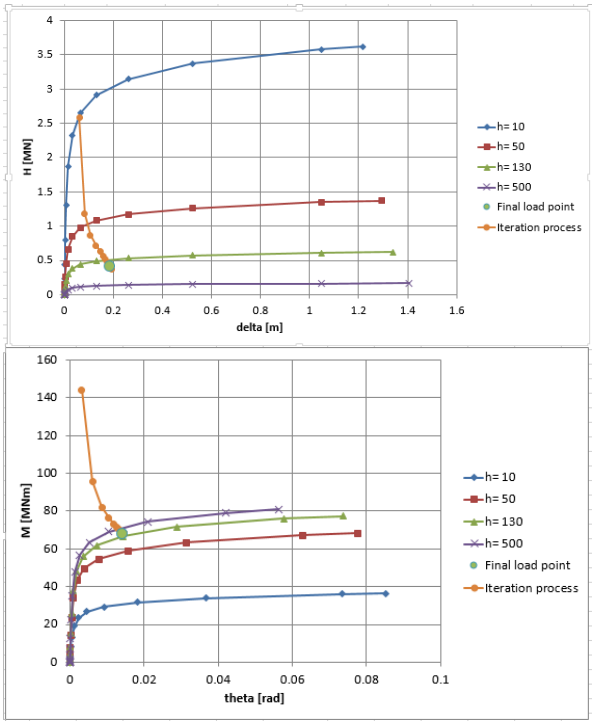

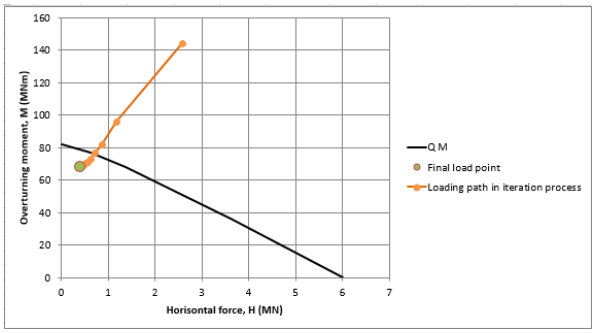

Figure 8. Results from modal analysis

If the convergence is not obtained, a new iteration is performed using the h_{dyn} as the new assumed loading ratio, h and the average mobilization degree of force and moment from the previous iteration to determine the stiffness's. Figure 8 illustrates the results of iteration process.

5 SHORTCOMINGS AND FUTURE DEVELOPMENTS OF THE MODEL

A macro-element model consisting of a yield surface and back-bone curves defining kinematic hardening rule for monotonic loading is presented. It can be used for static and dynamic soil-structure interaction analyses in frequency domain using equivalent, linear secant stiffness.
Adjustments are still required to account for effect of geometry aspect ratio L/D, non co-planar HM loads, gapping, etc. The main shortcoming of the model is that it can not incorporate the effect of load reversal.
The main task for future development of the model is the attempt to describe the elasto-plastic behaviour upon unloading and reloading. This will enable soil-structure interaction analyses of variable, cyclic loading and of dynamic analyses in time domain.

6 ACKNOWLEDGEMENTS

The authors wish to thank their colleagues at Industry Oil and Gas (IOG) Section of Geotechnical Department in Multiconsult for fruitful ideas and discussions during everyday design activity for offshore projects. The assistance from Dr. Steffen Giese, Head of the IOG Section, who encouraged and provided financial support for research work by internal funds, is gratefully acknowledged.

7 REFERENCES

Athanasiu, C., Shahrokhi, F. and Nalbant, R., M. (2008) Geotechnical Challenges of Earthquake Design according to NS3491-12. 15th Nordic Geotechnical Meeting, Sandefjord, Norway.

Gazetas, G. (2005) Foundation Vibrations. Chapter 15 in Foundation Engineering Handbook.

Houlsby, G.T., Ibsen, L.B. and Byrne, B.W. (2005) Keynote Paper: Suction caissons for wind turbines. ISFOG, 2005.

ISO 19901-4: 2003 Requirements for offshore structures. Part 4:Geotechnical and foundation design considerations.

Kay, S., & E. Palix (2011) Caisson capacity in clat: VHM resistance envelope-Part2: VHM envelope equation and design procedures. ISFOG 2011.

Kay, S. (2015) CAISSON_VHM: a program for caisson capacity under VHM load in undrained soils. ISFOG 2015.